RESIDUAL STRESS ANALYSIS IN METAL/CERAMIC FUNCTIONALLY GRADED MATERIALS

D. Dantz[1]), C. Genzel[1]), W. Reimers[1]), K.-D. Liss[2])

[1]) Hahn-Meitner-Institut Berlin
Glienicker Str. 100, 14109 Berlin, Germany
[2]) European Synchrotron Radiation Facility
BP 220, F-38043 Grenoble Cedex, France

ABSTRACT

Non-destructive diffraction experiments were performed on microwave sintered functionally graded materials (FGM) consisting of Ni and 8Y-ZrO_2 to analyse the residual stress distribution. In order to get information of the complete residual stress state in the near surface region as well as in the bulk of the material, complementary methods were applied. The residual stresses at the surface were investigated by the $\sin^2\psi$-method using conventional X-ray sources. For the interior of the material high energy synchrotron radiation allowing high spatial resolution were used. The stress state in the bulk of the material was found to be almost hydrostatic. It is related to the compositional distribution of the present phases, their volume fraction and their coefficients of thermal expansion. Additionally, the line broadening was analysed by a single-line method with respect to plastic deformation of the metallic phase, in order to characterise the microstructure of the samples.

1. INTRODUCTION

Ceramic/metal coatings are in use for a variety of applications such as thermal barrier, wear protection or electrically insulation. Due to the discontinuity of the materials properties high thermal residual stresses may arise near the interface area. These stresses can lead to plastic deformation of the metal phase, crack initiation in the ceramic or interfacial decohesion (Williamson et al [1]). In order to reduce these problems the materials concept of functionally graded materials (FGM) has been proposed, because they meet the demand for adjusting defined property gradients within technical parts. Due to a continuous variation of the properties residual stress concentrations can be avoided (Suresh and Mortensen [2]). But due to the mismatch of the coefficients of thermal expansion (CTE) and the elastic constants between the individual phases, micro residual stresses arise as a consequence of thermal or mechanical loads during manufacturing and under service conditions. These residual stresses are well-known to influence the mechanical properties of the device significantly, because they are often superimposed by load stresses during operation (Giannakopoulos et al [3]).

This paper deals with the non-destructive evaluation of the micro and macro residual stress distribution in Ni/8Y-ZrO_2 FGMs. The residual stress state in functionally graded materials depends strongly on the microstructure of the composite (network structure or dispersive in-

D. Dantz, Ch. Genzel, W. Reimers, K.-D. Liss: *"Residual Stress Analysis in Metal/Ceramic Functionally Graded Materials"*, The Sixth International Conference on Residual Stress (ICRS-6), IOM Communications, London, Vol. 1, (2000), pp. 717-724.

clusion), the overall thickness of the gradient as well as on the design of the compositional gradation and the thermal history (Dantz et al [4]). In order to improve the sintering process in one specimen, the ceramic phase was partially replaced by $ZrSiO_4$. The influence of the additional phase on both, the microstructure and the micro and macro residual stress distribution was analysed. The investigations at the surface were performed by the $\sin^2\psi$-method by means of conventional X-ray sources (Macherauch and Müller [5]), the experiments in the bulk of the material experiments were carried out using high energy X-ray diffraction (HXRD) (Reimers et al [6], Dantz et al [7]). In addition the line broadening was estimated by using the VOIGT function in a single-line method for profile analysis concerning the mean squared stresses $\langle e \rangle$ and the size of the crystallites (Langford [8]).

2. BASIC PRINCIPLES OF THE APPLIED DIFFRACTION METHODS

Residual Stress Analysis at the Near Surface Region

X-ray stress analysis (XSA) at the surface of polycrystalline materials by the classical $\sin^2\psi$-method is based on the determination of the lattice spacings $d(hkl)$ for different angle sets (φ,ψ) with respect to the sample system P. From the lattice strains $\varepsilon(hkl) = d(hkl)/d_0(hkl) - 1$ (d_0 – lattice spacing of the stress free state) obtained at various inclination angles ψ the corresponding stresses were calculated by linear regression (Macherauch and Müller [5]). In multiphase materials the average phase specific residual stresses $\langle\sigma\rangle_{\alpha,\beta}$ are accessible. The average with respect to the volume fraction yields the macro residual stresses $\sigma^I = V_\alpha\langle\sigma\rangle_\alpha + V_\beta\langle\sigma\rangle_\beta$ (V_α - volume fraction of the phase α, β). From the average phase specific and the macro residual stresses the micro residual stresses $\langle\sigma^{II}\rangle_{\alpha,\beta} = \langle\sigma\rangle_{\alpha,\beta} - \sigma^I$ can be derived.

Residual Stress Analysis in the Bulk of the Material

Due to the rather low absorption of high energy synchrotron radiation, penetration depths in the range of centimetres can be achieved and the experiments can be performed in the transmission mode. In Fig. 1 the experimental setup is shown. By means of narrow slits in the primary as well as in the secondary beam a sufficient small gauge volume for position resolved stress analysis in the bulk of the material is defined. In energy dispersive X-ray diffraction the correlation between the lattice spacings $d(hkl)$ and the corresponding energy peak $E(hkl)$ is obtained by $d(hkl) = hc/[2\sin\theta \cdot E(hkl)]$, where h is PLANCK's constant and c is the light velocity. The average values of the phase specific stresses $\langle\sigma_{ij}\rangle$ can be calculated according to

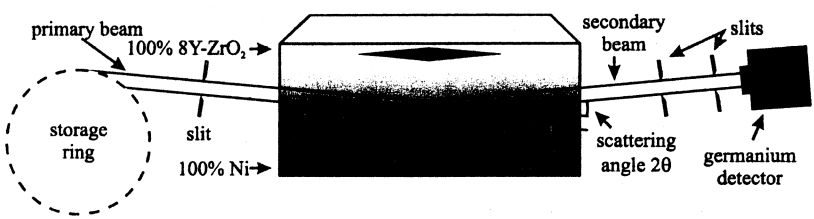

Fig. 1: Experimental setup for residual stress analysis using high energy synchrotron radiation (Dantz et al [7])

HOOKE's law for the triaxial stress state. Recording the complete energy spectrum available at some fixed detector position 2θ offers the possibility to include a series of reflections in the stress evaluation and, therefore enhances the reliability of the results (Dantz et al [6]).

Line Profile Analysis

The line profiles of diffraction patterns are influenced by instrumental broadening and by the microstructure of the crystals. The line breadth is affected by both, the size of the coherent reflecting domains as well as the micro strain in the crystal lattice. Assuming that the diffracted profile is a convolution of the reference and the physical profile, which can be described by a VOIGT-function, the single-line method was applied. This method is converted to the energy dispersive case. For details see Langford [8] and Otto [9].

3. EXPERIMENTAL

Samples

The samples of the material system Ni/8Y-ZrO_2($ZrSiO_4$) investigated consist of 11 sub-layers, in which the ceramic content was successively varied by steps of 10 vol.% from 0 to 100 vol.%. After milling of the individual powder mixtures in a planetary mill the powders with different ceramic and metal volume fraction were prepared by drying and sieving. The gradient is formed sub-layer by sub-layer by subsequent filling of a silicon mold with the individual powder mixtures. Then, after compacting by isostatic pressing, the graded powder specimens were pressureless sintered in a microwave field and subsequently cooled down to room temperature. Due to the different absorption of the microwave radiation by the ceramic and metal phase, a temperature gradient of 100-200°K from the ceramic to the metal side arises during the sintering process (Willert-Porada and Borchert [10]).

The parametric description of the phase distribution along gradient direction is described by the expression $V_\alpha = (x/t)^n$. V_α is the volume fraction of component α, t the thickness of the whole gradation and n denotes the distribution component. Specimens consisting of Ni/8Y-ZrO_2 were investigated, two of them with a non-linear gradation (n = 1,3 and n = 2, shown in Fig. 2a,), and one with a linear metal/ceramic gradation (n = 1, Fig. 2b), in which

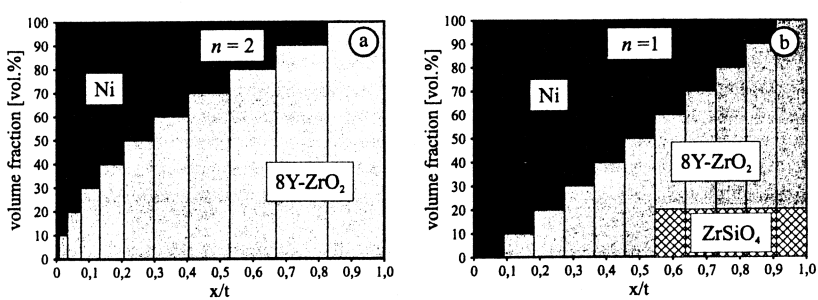

Fig. 2: Compositional distribution of the specimens: a) non-linear gradient, distribution exponent n = 2 b) linear gradation, partially substitution of 8Y-ZrO_2 by $ZrSiO_4$

the 8Y-ZrO_2 was partially substituted by $ZrSiO_4$ in the sub-layers with more than 50 vol.% ceramic content (Borchert and Willert-Porada [11]).

Diffraction Methods

The experiments using conventional X-ray sources were performed with CoKα-radiation and a Huber Ψ-diffractometer, which was equipped with a φ-rotation table as well as with a parallel beam unit consisting of a vertical soller-slit followed by (001)-LiF analysator in order to suppress fluorescence as well as the horizontal divergence of the diffracted beam for measurements at high ψ-tilt angles (77°). The measurements were performed at the Ni (222)-reflection ($2\theta \approx 123.3°$), at the 8Y-ZrO_2 (511)-reflection ($2\theta \approx 129.6°$) and at the $ZrSiO_4$ (312)-reflection ($2\theta \approx 63.1°$).

The investigations in the bulk of the materials using high energy synchrotron radiation were carried out at the beamline ID15/a at the European Synchrotron Radiation Facility (ESRF). An energy dispersive Ge-detector was used to record the diffraction pattern at a fixed angle of $2\theta = 7.6°$ within an energy range from 30 to 200 keV. Due to the high photon flux of the synchrotron radiation the gauge volume could be limited to 0.11 x 0.12 x 1.6 mm^3 by slits in the primary as well as in the secondary beam. The high spatial resolution allows measurements in each sub-layer perpendicular and parallel of the gradation direction. Recording the complete energy spectrum offers the possibility to use a series of reflections in the stress evaluation. The microstructure in the metal phase were investigated at the Ni-(222)-reflection by a single-line method of the profile analysis. The reference measurements were performed at the corresponding powder samples of each present phase. For the residual stress analysis in the interior as well as at the surface of the specimens the diffraction elastic constants (DEC) have been calculated by the KRÖNER-model (Kröner [12]).

4. RESULTS AND DISCUSSION

Near Surface Residual Stress Analysis

By preliminary measurements the in-plane stress state on top and bottom surface was proofed to be of rotational symmetry. The results for the top side (pure ceramic) and the bottom side of the graded plate (pure metal) are summarised in *Fig. 3*. On the macroscopic scale in both specimens, which were investigated, tensile residual stresses in the ceramic phase and compressive stresses in the metal phase are observed. This is in contrast to the expected macroscopic residual stress profile over the cross section due to the average CTE's of the individual sub-layers, which indicate tensile residual stresses in the metal rich parts of the component and compressive ones in the ceramic rich area. The origin of the observed stress profile becomes clear considering the temperature gradient during the sintering process. During cooling down an additional temperature difference of $\Delta T \approx 100\text{-}200°K$ occurs between the ceramic side (higher temperature) and the metal side. In the graded plate with a linear gradation the compressive stresses at the bottom surface are balanced by the tensile stresses in the ceramic rich region. Due to the thicker ceramic rich sub-layers in the specimen with a distribution exponent of $n = 2$ smaller tensile stresses are found. The smaller cross sections of the sub-layers on the metal rich side have to be compensated by tensile stresses of higher amount in comparison to the compressive macro residual stresses on the ceramic dominated zone.

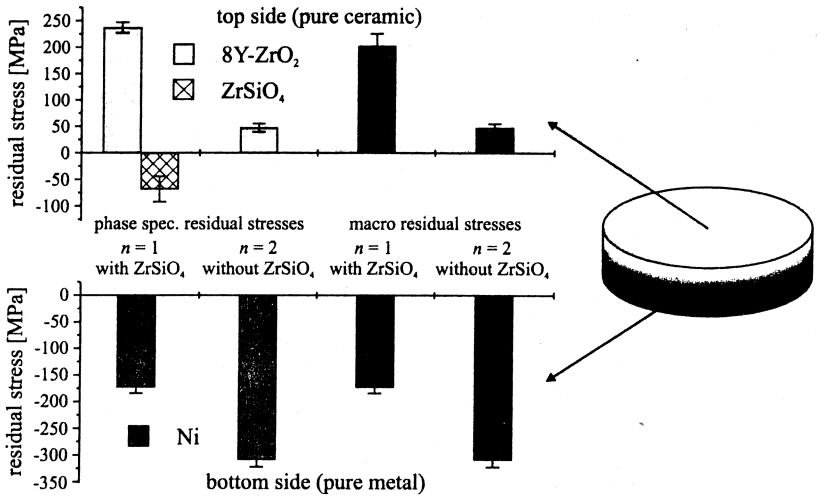

Fig. 3: Phase specific and macro residual stresses at the top and bottom side of the specimens with linear gradation and with an distribution exponent of n = 2.

Residual Stress Analysis in the Bulk of the Material

Prior investigations showed that the residual stress state parallel to the sub-layer interfaces is of rotational symmetry. In Fig. 4 the results of the residual stress analysis in the bulk of the sample in the material system Ni/8Y-ZrO_2($ZrSiO_4$) are presented. The out-of-plane stresses perpendicular to the interfaces have the same amount as the in-plane component of the phase specific residual stresses (Fig. 4a). Therefore, a hydrostatic residual stress state may be concluded for the interior of the material. Due to the very low coefficient of thermal expansion high compressive stresses are observed in the silicate phase. In the ceramic the phase specific stresses are compressive and decrease with increasing volume fraction. The high compressive stresses in the ceramic phases are partially compensated by tensile stresses in the metal phase. At low ceramic content they increase with decreasing metal volume fraction. But, at the admixture of $ZrSiO_4$ the phase specific residual stresses in the metal are reduced to values near 0 MPa.

Fig. 4b shows the micro and macro residual stress distribution in the specimen with a linear compositional gradient. The compressive macro residual stresses at high ceramic content are balanced by tensile macro stresses in the area with a small ceramic content. The phase specific micro residual stresses are a measure for the constrain between the present phases as well as for porosity and crack density. For that reason they influence the strength of a part decisively. In the present case they follow the thermal expansion behaviour prescribed by the individual CTE of the present phases, i. e. the lower the CTE the higher become the compressive stresses of the corresponding phase relative to the other components and vice versa. The difference between the micro stresses of the 8Y-ZrO_2 and the metal phase remain nearly constant over a wide range of the compositional gradation. At the admixture of the $ZrSiO_4$ this difference is reduced significantly, which can be attributed to cracks in the ceramic rich area.

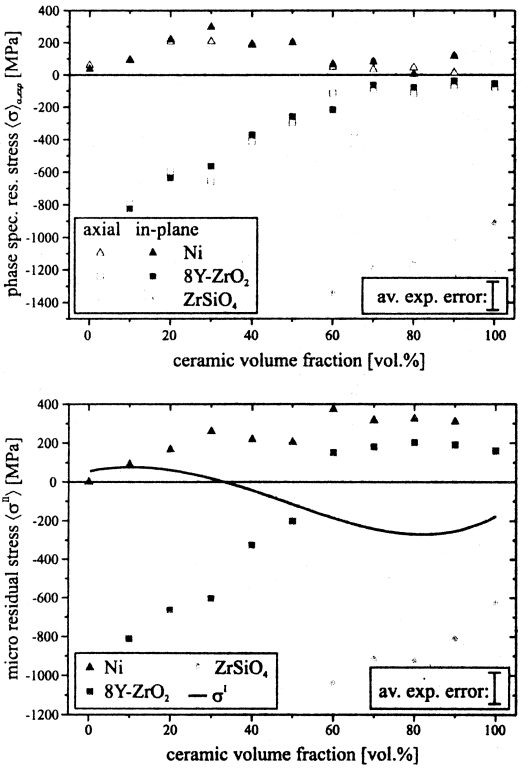

Fig. 4: Residual stress state in the bulk of the sample in the material system Ni/8Y-ZrO_2 ($ZrSiO_4$):
a) phase specific residual stress distribution,
b) macro and micro residual stress distribution

The residual stress distribution in the specimen with the non-linear compositional gradation (n = 1,3) is shown in Fig. 5. The results are in good agreement to the findings obtained for the FGM with the silicate admixture and the linear gradation. With regard to the phase specific stresses this holds true for both the run as well as the absolute amount of the profiles (Fig. 5a). On the macroscopic scale even on the metal rich side compressive stresses are observed (Fig. 5b). This finding is in agreement with the near surface results, which gave compressive stresses up to 300 MPa. They can be attributed to the temperature gradient during sintering. The tensile stresses on the metal side and the compressive stresses in the ceramic rich region, which were observed in the sample with linear gradation, in this case are superimposed by the stresses generated by the inhomogeneous sintering temperature. With increasing distribution exponent the cross sections of the metal rich sub-layers decrease and, therefore, the compressive macro stresses have to increase. The micro residual stresses are consistent with the individual CTEs of the present phases. On the metal rich side the difference between the micro stresses of the metal and ceramic component are nearly constant over almost the whole range of the cross section comparable to the specimen with the silicate admixture.

As shown in Fig. 5a, the tensile phase specific residual stresses in the metal phase are nearly constant for a ceramic content of about 30 vol.% up to amounts of 80 vol.%. This indicates a relaxation of the stresses due to plastic deformation of the metal component. In order

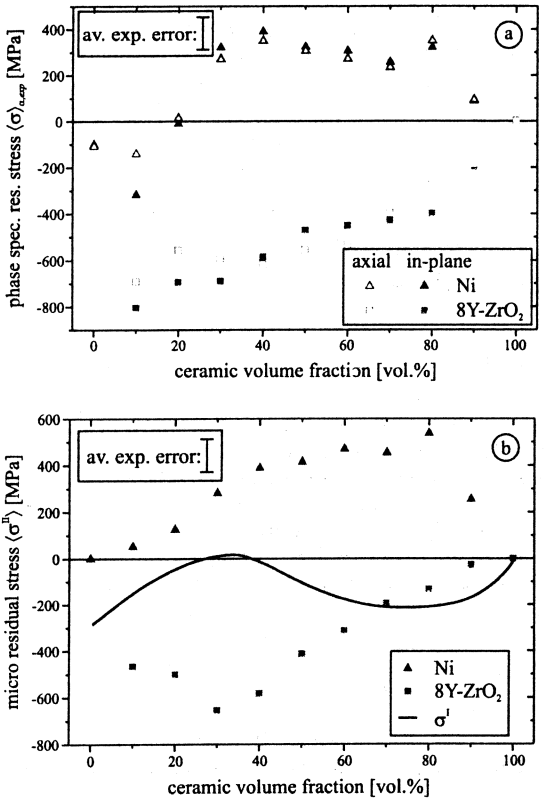

Fig. 5: Residual stress state in the bulk of the sample in the material system Ni/8Y-ZrO2 with a distribution exponent of n = 1,3:
a) phase specific residual stress distribution
b) macro and micro residual stress distribution

to analyse this phenomenon, the line broadening was investigated by a single-line method, which was converted to the energy dispersive case. The results are shown in Fig. 6. The CAUCHY contribution of the corrected integral breadth β_{fC}, which is predominantly affected by size effects (Langford et al [13]), remains nearly constant over the whole cross section of the graded plate. On the other hand, the GAUSS contribution β_{fG} which mainly reflects the line broadening due to the mean squared micro strain $\langle e \rangle$ caused by lattice defects such as dislocations and stacking faults, shows higher values. With decreasing metal volume fraction the GAUSSian integral breadth increases, which is an additional indication for a stress relaxation in the metal phase due to plastic deformation.

5. CONCLUSIONS

The residual stress state in microwave sintered metal/ceramic graded specimens can be characterised by different diffraction methods. It is shown, that high energy X-ray diffraction with its high spatial resolution is a well suited method for the evaluation of the residual stress state in the bulk of FGMs even with steep compositional gradients. The results show, that the macro residual stress state is influenced by different CTEs, which leads to compressive

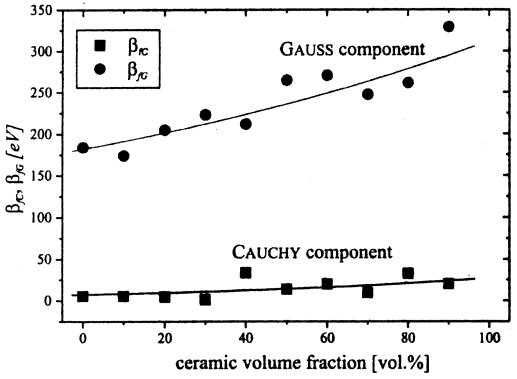

Fig. 6: Separation of the CAUCHY and GAUSS contribution of the integral breadth, β_{fC} and β_{fG}, of the Ni (222)-reflection corrected by the reference

stresses on the ceramic rich side and tensile stresses on the metal side. These stresses are superimposed by those due to the individual shape of the gradation and the temperature distribution during the manufacturing process. The phase specific micro residual stresses are consistent with CTEs of the individual phases. They are also significantly affected by additional phases ($ZrSiO_4$). Furthermore, the findings from the profile analysis show, that the tensile stresses in the metal phase are reduced by plastic deformation. The results also suggest additional investigations with respect to the reduced tensile stresses in the Ni at the admixture of the silicate phase.

ACKNOWLEDGEMENT

The authors are obliged to Prof. Dr. M. Willert-Porada and Dr. R. Borchert for the provision of the specimens. The financial support of the German Research Foundation (DFG) is gratefully acknowledged, reference no. Re 688/23, 1-3.

REFERENCES

[1] Williamson R L, Rabin B H, Drake J T, J. Appl. Phys. 74 (1993) 1310-20
[2] Suresh S, Mortensen A, Int. Mater. Rev. 42/3 (1997) 85-116
[3] Giannakopoulos A E, Suresh S, Finot M, Olsson M, Acta Metal. Mater. 43/4 (1995) 1335-1354
[4] Dantz D, Genzel Ch, Reimers W, Mater. Sci. Forum 308-311 (Proc. 5th Int. Symp. on FGM '98, Dresden, Germany) (1998) 829-836
[5] Macherauch E, Müller P, Z. angew. Phys. 13/7 (1961) 305-312
[6] Reimers W, Broda M, Brusch G, Dantz D, Liss K-D, Pyzalla A, Schmackers T, Tschentscher T, J. Non-Dest. Eval. 17/3 (1998) 129-140
[7] Dantz D, Genzel Ch, Reimers W, Proc. of Euromat '99 Munich (1999), in press
[8] Langford J I, J. Appl. Cryst. 11 (1978) 10-14
[9] Otto J W, J. Appl. Cryst. 30 (1997) 1008-1015
[10] Willert-Porada M A, Borchert R; Proc. 4th Int. Symp. on FGM '96 Tsukuba, Japan (1996) 349
[11] Borchert R; Willert-Porada M A, Proc. 100th ACERS-Meeting (1998)
[12] Kröner E, Z. f. Phys. 151 (1958) 504
[13] Langford J I, Delhez R, de Keijser T H; Mittemeijer E J, Aust. J. Phys. 41 (1988) 173-187